Journal of Babylon University/Engineering Sciences/ No.(4)/ Vol.(24): 2016

Derivation of Output Power of Induction Heater Model

Riyadh K. Chillab
AL Mamon University College – Department of Electrical Power Technical Engineering
inductionm@yahoo.com

Abstract

The work is concerned with the study of the single phase cylindrical induction heating systems and derive equation power. The presented analysis is analytical and a multi-layer model using cylindrical geometry which is used to obtain the theoretical results.

To validate the theoretical results, a practical model is constructed, tested and the results are compared with the theoretical ones. Comparison showed that the adopted analytical method is efficient in describing the performance of such induction heater systems.

Key words : induction heating, magnetic fields , eddy currents.

الخلاصة

يختص هذا البحث في الدراسة النظرية و العملية لتحليل أنظمة التسخين الحثي أحادية الطور لقطع معدنية إسطوانية الشكل وأشتقاق معادلة القدرة الخارجة لهذه الانظمة . تم تصنيع نموذج عملي لأجراء الفحوصات العملية لهذا النوع من المسخنات الحثية.

إن الطريقة التي تم إستخدامها نظريا لتحليل هذا المسخن هي طريقة تحليلية تعرف بنظرية الطبقات المتعددة بإستخدام المحاور الإسطوانية.

أجريت المقارنة بين النتائج النظرية و العملية، وبينت هذه المقارنة كفاءة الطريقة المستخدمة نظريا و وصفت إداء هذا النوع من المسخنات الحثية.

الكلمات المفتاحية : التسخين الحثي، المجالات المغناطيسية، التيارات الدوامة

Symbols List

B	magnetic flux density, T
E	electric field, V/m
H	magnetic field, A/m
P_{iu}	power induced in the work-piece, W
I_{max}	peak current, A
J'	amplitude of current density, A
l	coil length, m
N	number of turns
F	supply frequency, Hz
r,θ,z	Sub-script for coordinates
μ	permeability, H/m
σ	conductivity, s/m

1. Introduction

The first target of this work is to propose a general analytically model for the system Fig.(1) using the existing topology for single-phase excitation in the axial direction. As a second object, the paper involve the multi-layer with a current sheet representation to calculate the flux density components and induced power in the work-piece.

The primary coil construction may be explained in a similar method with the help of Fig.(2) which shows the cylindrical solenoidal coil system divide axially.

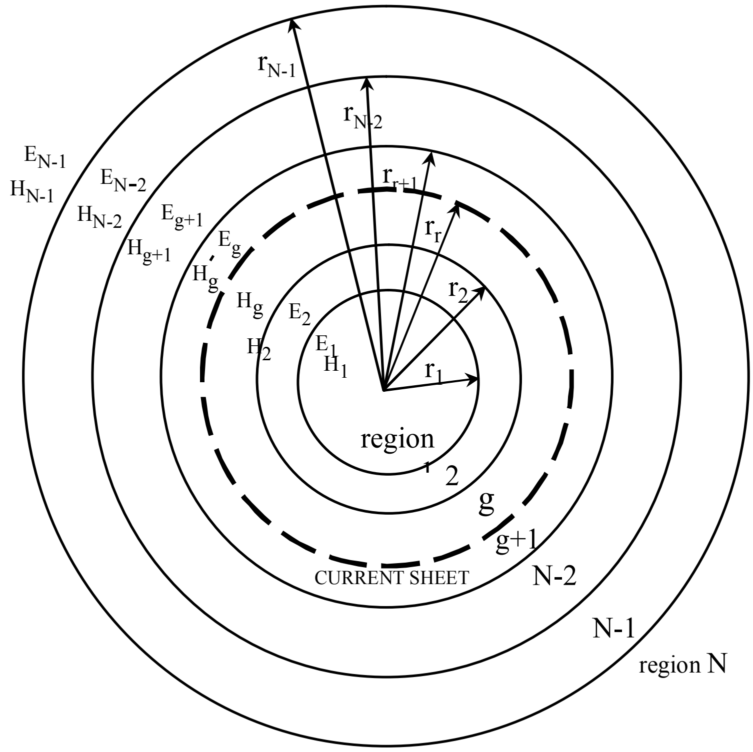

Fig.(1) Cross-sectional of multi-cylinders induction heater system

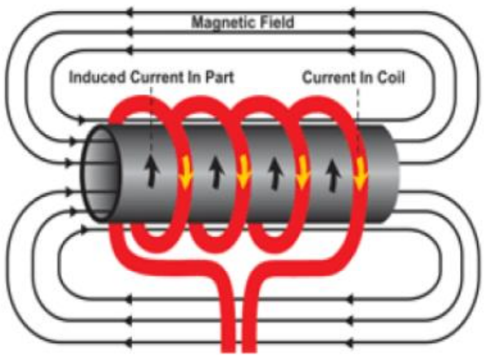

Fig.(2) A coil with a certain number of turns

2. Mathematical Representative

A multi-area problem is resolve. The form is given to be a set of infinite long cylinders, with a radial thin and axial infinite current sheet excitation of radius r_g. It is assumed that magnetic field saturation is deleted (Davies and Simpson 1979).

Maxwell's equations for any area in the model are

$$\text{curl } H = J \tag{1}$$

$$\text{curl } E = -\frac{\partial B}{\partial t} \tag{2}$$

$$\text{div } E = 0 \tag{3}$$

$$\text{div } B = 0 \tag{4}$$

$$\text{div } J = 0 \tag{5}$$

$J = \sigma E$ (6)
$B = \mu H$ (7)

The boundary conditions are.
1. The radial component of flux density is continuous across a boundary.
2. The radial component of line current density is assumed to be zero.
3. The axial component of magnetic field strength is continuous across a boundary, but allowance for the current sheet should be taken into account.

3. Theoretical method

3.1 The field equations of a normal area

The field equations of a normal region are deduced. Assuming that all fields vary as $e^{j(\omega t)}$(Bianchi and Dugiero 1995), and removel this factor from all the field expressions that follow.

The r-axis form two sides of equation (2) obtain

$$\frac{\partial E_\theta}{\partial z} = j\omega\mu H_r$$

and

$$H_r = 0 \quad (8)$$

For the z-axis form two sides of equation (2), one can get

$$\frac{1}{r}\frac{\partial r E_\theta}{\partial r} = -j\omega\mu H_z \quad (9)$$

By two equations (1) and (6) and using the θ-axis from two sides, get

$$-\frac{\partial H_Z}{\partial r} = \sigma E_\theta \quad (10)$$

Then, rearranging, equation (10) may be written

$$r^2\frac{\partial^2 E_\theta}{\partial r^2} + r\frac{\partial E_\theta}{\partial r} - \left(\alpha^2 r^2 + 1\right)E_\theta = 0 \quad (11)$$

The disentanglement is given by

$$E_\theta = AL_1(\alpha r) + DL_2(\alpha r) \quad (12)$$

Where

$$\alpha^2 = j\omega\mu\sigma$$

L_1 and L_2 are the modified Bessel equations of a first request of general complex proof. A and D are constants to be calculate from boundary conditions.

From equations (2), (7) and (12), can be obtained

$$H_z = j\frac{\alpha}{\omega\mu}\left[AL_{01}(\alpha r) + DL_{02}(\alpha r)\right] \quad (13)$$

3.2 Field computation at the area boundaries

Fig.(3-a) gives a general area n, where $E_{\theta,n}$ with $H_{z,n}$ are the field parts at the above boundary of a area, and $E_{\theta,n-1}$ with $H_{z,n-1}$ are the values of equivalent at the down boundary.

From equations (12) and (13), they can be shown that

$$E_{\theta,n} = AL_1(\alpha_n r_n) + DL_2(\alpha_n r_n) \quad (14)$$

and

$$H_{z,n} = j\frac{\alpha_n}{\omega\mu_n}\left[AL_{01}(\alpha_n r_n) - DL_{02}(\alpha_n r_n)\right] \qquad (15)$$

By replacing (r_n) in the above equations by (r_{n-1}). The forms $H_{z,n-1}$ with $E_{\theta,n-1}$ can be found

For areas where n ≠ 1 and N,

$$\begin{bmatrix} E_{\theta,n} \\ H_{z,n} \end{bmatrix} = [Q_n]\cdot\begin{bmatrix} E_{\theta,n-1} \\ H_{z,n-1} \end{bmatrix} \qquad (16)$$

$[Q_n]$ is the matrix of transfer (Alwash 1972, Al-Shammari 2009) for area n, and is obtain by

$$[Q_n] = \begin{bmatrix} a_{1n} & a_{2n} \\ a_{3n} & a_{4n} \end{bmatrix} \qquad (17)$$

The elements for the matrix of transfer are determine in the appendix page, the rates of E_θ and H_z at the down boundary of a area, the rates of E_θ and H_z at the above boundary can be found by using the matrix of transfer . At boundaries where without excitation current sheet exists E_θ and H_z are free value, if two areas are considered to have without current sheet at their boundary, knowing the rates of E_θ and H_z at the beginning of the first area, values of E_θ and H_z at the end of the second area can be found by using two matrices of transfer.

The current sheet to be at radius r_g,

$$H'_{z,n} - H_{z,n} = 0 \qquad g \neq n \qquad (18)$$

and

$$H'_{z,n} + J = H_{z,n} \qquad g = n \qquad (19)$$

$H_{z,n}$ is an axial magnetic field intensity below a boundary, and $H'_{z,n}$ is a magnetic field intensity above a boundary.

$$\begin{bmatrix} E_{\theta,N-1} \\ H_{z,N-1} \end{bmatrix} = [Q_{N-1}]\cdot[Q_{N-2}]\cdots\cdots[Q_{g+1}]\begin{bmatrix} E_{\theta,g} \\ H_{z,g} - J' \end{bmatrix} \qquad (20)$$

and

$$\begin{bmatrix} E_{\theta,g} \\ H_{z,g} \end{bmatrix} = [Q_g]\cdot[Q_{g-1}]\cdots\cdots\cdots[Q_2]\begin{bmatrix} E_{\theta,1} \\ H_{z,1} \end{bmatrix} \qquad (21)$$

If area N is now represented , as Fig. (3-b),

$L_1(\alpha r) \rightarrow \infty$ and $(r \rightarrow \infty)$.

from equation (14) and (15) one may get that A=0

$$E_{\theta,N-1} = DL_1(\alpha_N r_{N-1}) \qquad (22)$$

and

$$H_{z,N-1} = -j\frac{\alpha_N}{\omega\mu_N}DL_{01}(\alpha_N r_{N-1}) \qquad (23)$$

The first area (1), then

$L_1(\alpha r) \rightarrow \infty$ and $(r \rightarrow 0)$

From equation (14) and (15) one may get D=0

$$E_{\theta,1} = AL_1(\alpha_1 r_1) \qquad (24)$$

and

$$H_{z,1} = j\frac{\alpha_1}{\omega\mu_1} AL_{01}(\alpha_1 r_1) \qquad (25)$$

The field parameters at the boundaries of areas (1) with (N) still contain constants, the results of E_θ to H_z at these boundaries contain no constants, and it is only these results that are needed for a full solution. The next part shows how this may be accomplished. The results of E_θ to H_z have been termed the impedance of surface (Freeman and Smith 2009).

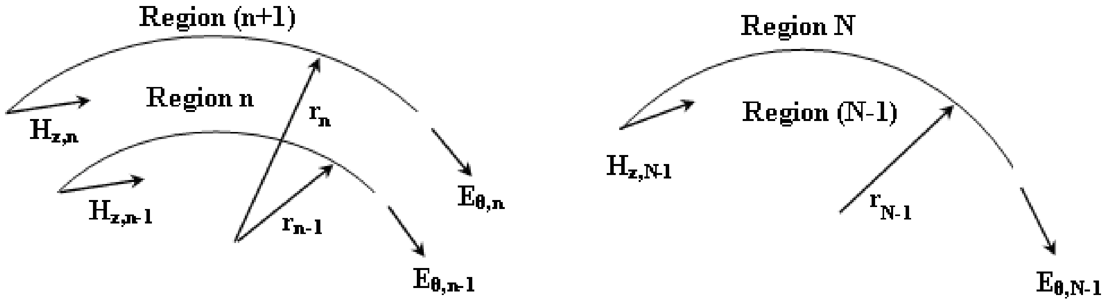

Fig.(3): The mathematical form
(a) General area n (b) End area N

3.3 impedance of Surface

The impedance of surface out at a boundary of radius r_s is defined as (Greig and Freeman 1967)

$$Z_{s+1} = \frac{E_{\theta,s}}{H'_{z,s}} \qquad (26)$$

and the impedance of surface in a boundary is defined as(Greig and Freeman 1967)

$$Z_s = -\frac{E_{\theta,s}}{H_{z,s}} \qquad (27)$$

Using the procedure given in (Greig and Freeman 1967) and the rates of $E_{\theta,N-1}$, $H_{z,N-1}$, $E_{\theta,1}$, $H_{z,1}$ and that of (a_{1n}, a_{2n}, a_{3n} and a_{4n}) as given in the appendix page , it can be shown that

$$Z_i = \frac{Z_g Z_{g+1}}{Z_g + Z_{g+1}} \qquad (28)$$

Z_i is the impedance of surface at the field of sheet, and Z_{g+1} and Z_g are the impedance of surface looking in and out at the sheet (Freeman 1968).

To find Z_g and Z_{g+1} using equations (28) and (27), and with arranging to obtain

$$Z_i = \frac{-E_{\theta,g}}{H_{z,g} - H'_{z,g}} \qquad (29)$$

By equation (20)

$$J = H_{z,g} - H'_{z,g} \qquad (30)$$

By using equation (30)

$$Z_i J = -E_{\theta,g} \qquad (31)$$

The input impedance at the sheet (Z_i) has been calculated .This means that all the field axis can be found by using the equations (28), (21) and (22).

3.4 output power

The time total power passing through a surface is obtain (Alwash and Muhsen 2003), (Eastham and Alwash 1972)

$$P_{in} = m\frac{1}{2}\mathrm{Re}\left(\overline{E}_{\theta} \times \overline{H}_{z}^{*}\right) \quad (\mathrm{w/m^2}) \qquad (31)$$

by equations. (27), (30) and (31), can be found that the total work-piece power is

$$P_{iu} = 3.5\left|J'\right|^{2}(Z_{in}) \quad (\mathrm{w}) \qquad (32)$$

4. Experimental Analysis

4.1 Model description

Fig.(4) showed the practical test rig. The coil was wound circularly on a tube of plastic. Since the core has no backing iron then the primary circuit is of the open type form. The coil is apply to a variable voltage supply. It is worth mentioning that this coil represent the heating part of the system (heater). The heater was then mounted and fixed on a board using a suitable mechanical structure. This enables fine adjustment for a uniform air-gap surrounding the work-piece that represents the load . The type of the work-piece used is a solid aluminum cylinder. The magnetic circuit for this material provides the required flux paths. The conductivity of the work-piece was measured using standard DC measurement. Table 1 shows the parameters of the practical model.

To determine the magnetic flux density on the work-piece surface, simple type of independent probe (search coil) was used.

Fig.(4) Photograph of the experimental model

4.2 Load power measurement

The load power was measured experimentally as follows:

a. The input power to the heater was measured by using wattmeter.

b. coil current was measured using an ammeter. Then, the copper loss for the coil was calculated, (Bowden and Davies 1982), (Schulze and Wang 1996) as

$$P_{co} = I_{ci}^{2} R_{ci} \quad (\mathrm{w}) \qquad (33)$$

Where

P_{co} : Copper loss of coil conductors, (w).

I_{ci} : Primary current, (A).

R_{ci} : Resistance of primary coil, (Ω)

c. The load power in work-piece was found by subtracting the copper losses from the input power, as follows

$$P_{kkh} = P_{tot} - P_{co} \quad (w) \tag{34}$$

Where

: Load power in work-piece, (w).

: Total input power, (w).

5. Conclusion

The analytic undoing by the multilayer theory has been used for the analysis of induction heater system for single-phase excitation. The given analysis is quite general in that it lends itself to the analysis of induction heater.

The shown results explain clear that the theoretical results get together well with the practical ones. This may be regarded as fair to the method adopted for the analysis in this work.

Table(2) shows the comparison between theoretical and practical results. It's clear from the results that the multilayer theory and the practical model show good method

6. Appendix

6.1 Derive elements of matrix

$$a_{1n} = \frac{r_{n-1}}{r_n} \tag{35}$$

$$a_{2n} = \frac{j\omega\mu_n}{2r_n}\left(r_n^2 - r_{n-1}^2\right) \tag{36}$$

$$a_{3n} = 0 \tag{37}$$

$$a_{4n} = 1 \tag{38}$$

Table (1) Experimental model parameters

Parameter/Characteristic	Value
Coil turns	3500
Coil inner diameter (mm)	50
Frequency (Hz)	50
Air-gap length (mm)	5
Primary conductor wire gauge	SWG 19.5
Charge length (mm)	700
Charge radius (mm)	20
Charge conductivity (s/m)	3.4×10^{7}
Charge relative permeability	1
Exciting current (A)	Variable

Table (2) Comparison between experimental and theoretical results for a charge power

Primary current of coil (A)	Charge power (w) experimental	Charge power (w) theoretical	Relative error
1	169.5	176.9	0.043
2	695	707.8	0.018
3	1583	1592.6	$6*10^{-3}$
4	2824	2831.3	$2.5*10^{-3}$
5	4404	4423.9	$4.5*10^{-3}$
6	6350	6370.5	$3.2*10^{-3}$
7	8645	8671	$3*10^{-3}$
8	11301	11325.4	$2.1*10^{-3}$
9	14300	14333.7	$2.3*10^{-3}$
10	17650	17695.9	$2.6*10^{-3}$

References

Davies, E.J. and Simpson, P.G.,1979,"Induction Heating Hand book" London Mc Graw Hill, (U.K.).

Bianchi, N. and Dughiero,F.,1995,“Optimal Design Techniques Applied to Transverse-Flux Induction Heating Systems,” IEEE Transactions on Magnetics,Vol. 31, No. 3, pp. 1992-1995.

Alwash, J.H.,1972,“Analysis and Design of Linear Induction Machines”; Ph.D. Thesis, Imperial College, London University, U. K.

Al-shammari, R. K., 2009,"Analysis of traveling wave cylindrical induction heating systems”; M.Sc. Thesis, Elect. Eng. Dept., College of Engineering, University of Baghdad.

Freeman, E.M., and Smith, B. E., 1970,“Surface impedance method applied to multilayer cylindrical induction devices with circumferential exciting currents”; Proc. IEE, vol. 117, No. 10, pp 2012-2013.

Greig, J., and Freeman, E.M.,1967,“Traveling wave problem in electrical machine”; Proc. IEE, vol. 114, pp. 1681-1683.

Freeman,E.M.,1968,“Traveling waves in induction machines: input impedance and equivalent circuits”; Proc. IEE, vol. 115, No. 12, pp. 1772-1776.

Alwash, J. H., Muhsen, A. D., and Abdi, A. S., 2003,“Helical motion tubular induction motor”; IEEE Trans. Energy Conv., vol. 18, No. 3, pp. 362-369.

Eastham, J. F., and Alwash, J. H.,1972,“Transverse-flux tubular motors”; Proc. IEE, vol. 119, No. 12, pp. 1709-1718.

Bowden,A.L.,Davies,E.J.,1982,"Travelling wave induction heaters:design consideration", BNCE-UIE Electroheal for Metals Conference, cnmbridge, England.

Schulze, D., and Wang, Z., 1996“Developing an Universal TFIH Equipment Using 3D Eddy Current Field Computation,” IEEE Transactions on Magnetics, Vol. 32, No. 3, pp. 1609-1612.